Collaborative Transportation of a Bar by Two Aerial Vehicles with Attitude Inner Loop and Experimental Validation

Pedro O. Pereira and Dimos V. Dimarogonas

Abstract

We propose a control law for stabilization of a bar tethered to two aerial vehicles, and provide conditions on the control law's gains that guarantee exponential stability of the equilibrium. Given the proposed control law, we analyze the stability of the equilibrium in three separate parts. In the first, the system is modeled assuming that the UAVs are fully actuated, and we verify that the equilibrium is exponentially stable. In the second part, the system is modeled assuming that the UAVs have an attitude inner loop, and we provide a lower bound on the attitude gain for which exponential stability of the equilibrium is preserved. In the third part, we add an integral action term to the control law, so as to compensate for battery drainage and model mismatches, such as an unknown bar mass. We present an experiment that demonstrates the stabilization and that validates the robustness of the proposed control law.

I. Introduction

Automated inspection and maintenance of aging infrastructures is a challenging task, and aerial vehicles provide a platform to partially solve and accomplish such task [1]. Vertical take off and landing rotorcrafts, with hover capabilities, and in particular quadrotors, form a class of underactuated vehicles whose popularity stems from their ability to be used in relatively small spaces, their reduced mechanical complexity, and inexpensive components [2], [3].

While there is noteworthy research on using quadrotors to perform specific tasks such as vision aided flying [4], arm-endowed aerial control [5] and flying with wind [6], in this paper we focus on transportation with quadrotors. Transportation by aerial vehicles is an important task in the scope of inspection and maintenance of infrastructures, and it forms a class of underactuated systems for which trajectory tracking control strategies are necessary [7]. To be specific, the system we focus on is composed of a one dimensional bar and two quadrotors attached to that bar by cables, and one of the control challenges lies in dampening the sway of the bar pose (position and attitude) with respect to the quadrotors.

Different slung load systems and related control strategies have been studied and proposed. Differential flatness has been explored for the purposes of control and motion planning of a single point mass load [8]–[11], while dynamic programming has also been used for trajectory planning [12], with the goal of minimizing the load swing. Adaptive controllers have been proposed which compensate for different unknown parameters [13]–[15], such as a variable center of gravity, an unknown load mass or a constant input disturbance. Vision has also been used to determine the pendulous mode frequency and thereby the cable length [16]. Load lifting by multiple aerial vehicles is also found in [17]–[20]. In particular, in [17], the relations in static equilibrium for a rigid body tethered to aerial vehicles are analyzed; in [18], [19] a controller is designed for three of more vehicles transporting a rigid body; and in [20] a control platform, including information exchange between the aerial vehicles, is developed and experimentally tested.

In this manuscript, we propose a control law with the objective of steering the bar to a desired pose, i.e., a desired position in the three dimensional space and a desired unit vector attitude. Linearization is used to infer exponential stability of the equilibrium, and conditions on the gains are provided for which exponential stability is guaranteed, in a similar approach to [21], [22]. Our main contributions lie in *i)* providing tight bounds on the gains such that exponential stability is guaranteed in the case where the aerial vehicles have an attitude inner loop, whose gain we cannot control; *ii)* in including an integral action term in the control law for compensating for battery drainage and model mismatches (such as an unknown bar mass), and providing tight bounds on the integral gains such that exponential stability is guaranteed; and *iii)* to experimentally validate the proposed control strategy.

The remainder of this paper is structured as follows. In Section III, the model of the quadrotors-bar system is described, and in Section IV the control law is provided. In Section V, we present conditions under which specific matrices, used in later sections, are Hurwitz. In Section VI we provide a strategy for analyzing unit vector dynamics under a linearization procedure. In Sections VII, we compute the Jacobian associated to the equilibrium, and verify it is Hurwitz. In Section VIII, we include the UAVs attitude inner loop, and in Section IX we include the integral action; in both cases, we provide conditions under which the Jacobian remains Hurwitz. Finally, in Section X, we present illustrative experimental results.

The authors are with the School of Electrical Engineering, KTH Royal Institute of Technology, SE-100 44, Stockholm, Sweden. {ppereira, dimos}@kth.se. This work was supported by the EU H2020 Research and Innovation Programme under GA No.644128 (AEROWORKS), the Swedish Research Council (VR), the Swedish Foundation for Strategic Research (SSF) and the KAW Foundation.

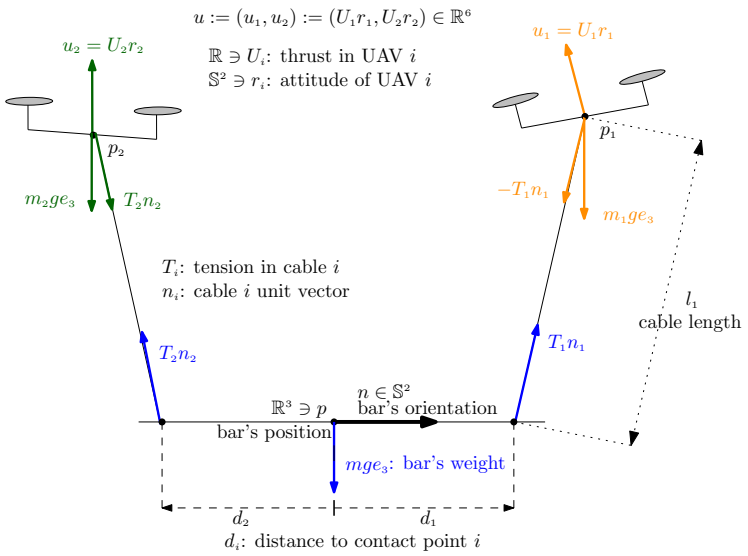

Fig. 1: Modeling of quadrotors-bar system

II. Notation

The map $\mathcal{S} : \mathbb{R}^3 \ni x \mapsto \mathcal{S}(x) \in \mathbb{R}^{3\times 3}$ yields a skew-symmetric matrix and it satisfies $\mathcal{S}(a)\, b = a \times b$, for any $a, b \in \mathbb{R}^3$. $\mathbb{S}^2 := \{x \in \mathbb{R}^3 : x^T x = 1\}$ denotes the set of unit vectors in $\mathbb{R}^3$. The map $\Pi : \mathbb{S}^2 \ni x \mapsto \Pi(x) := I_3 - xx^T \in \mathbb{R}^{3\times 3}$ yields a matrix that represents the orthogonal projection onto the subspace perpendicular to $x \in \mathbb{S}^2$. We denote $A_1 \oplus \cdots \oplus A_n$ as the block diagonal matrix with block diagonal entries A_1 to A_n (square matrices). Given $\bar{\sigma} > 0$, we denote $\sigma(\cdot, \bar{\sigma}) : \mathbb{R} \ni x \mapsto \sigma(x, \bar{\sigma}) := \bar{\sigma} \frac{x}{\sqrt{\bar{\sigma}^2 + x^2}} \in (-\bar{\sigma}, \bar{\sigma})$, as a saturation function bounded by $\bar{\sigma}$; and $\sigma^{-1}(\cdot, \bar{\sigma}) : (-\bar{\sigma}, \bar{\sigma}) \ni y \mapsto \sigma^{-1}(y, \bar{\sigma}) := \bar{\sigma} \frac{y}{\sqrt{\bar{\sigma}^2 - y^2}} \in \mathbb{R}$ as its inverse. We denote by $e_1, \cdots, e_n \in \mathbb{R}^n$ the canonical basis vectors in $\mathbb{R}^n$; when clear from the context, n is omitted. For some set A, id_A denotes the identity map on that set. Given some normed spaces A and B, and a function $f : A \ni a \mapsto f(a) \in B$, $Df : A \ni a \mapsto Df(a) \in \mathcal{L}(A, B)$ denotes the derivative of f. Given two matrices A and B, $A \simeq B :\Leftrightarrow A = PBP^{-1}$ for some invertible matrix P. Given a manifold A, $T_a A$ denotes the tangent set of A at some $a \in A$.

III. Problem Description

Consider the system illustrated in Fig. 1, with two aerial vehicles (in particular quadrotors), a one dimensional bar and two cables connecting the aerial vehicles to distinct contact points on the bar. Hereafter, and for brevity, we refer to this system as quadrotors-bar system. We denote by $p_1, p_2, p \in \mathbb{R}^3$ the quadrotors' and the bar's center of mass positions; by $v_1, v_2, v \in \mathbb{R}^3$ the quadrotor's and the load's center of mass velocities; by $n, \omega \in \mathbb{R}^3$ the bar's orientation and angular velocity; by $m_1, m_2, m > 0$ the quadrotors' and bar's masses; by $J > 0$ the bar's moment of inertia (w.r.t. the bar's center of mass); by $l_1, l_2 > 0$ the cables' lengths; and, finally, by $d_1, d_2 \in \mathbb{R}$ the contact points on the bar at which the cables are attached to. Finally, we denote by $u_1, u_2 \in \mathbb{R}^3$ the quadrotors' input forces, which we assume are inputs to the quadrotors-load system. Later, in Section VIII, we consider the effect of the attitude inner loop on the stability of the equilibrium, and therefore, in that Section, we also consider the quadrotors attitude, denoted by $r_1, r_2 \in \mathbb{S}^2$. Consider then the state space

$$\begin{aligned} \mathbb{Z} := \big\{ (p, n, p_1, p_2, v, \omega, v_1, v_2) \in (\mathbb{R}^3)^8 : & n^T n = 1, n^T \omega = 0, \\ & (p_i - (p + d_i n))^T (p_i - (p + d_i n)) = l_i^2, i \in \{1, 2\}, \\ & (v_i - (v + d_i \mathcal{S}(\omega)\, n))^T (p_i - (p + d_i n)) = 0, i \in \{1, 2\} \big\}. \end{aligned} \tag{1}$$

which encapsulates the constraints illustrated in Fig. 1. Specifically, the constraints in (1) imply that the bar's attitude n is given by a unit vector and the bar's angular velocity ω is orthogonal to that unit vector (rotations around the bar itself do not affect the bar's attitude); and that the distance between each contact point on the bar and the corresponding quadrotor is constant and equal to the corresponding cable length. We always decompose a $z \in \mathbb{Z}$ and a $u \in \mathbb{R}^6$ in the same way, namely

$$\begin{aligned} & z \in \mathbb{Z} :\Leftrightarrow (p, n, p_1, p_2, v, \omega, v_1, v_2) \in \mathbb{Z}, \\ & u \in \mathbb{R}^6 :\Leftrightarrow (u_1, u_2) \in \mathbb{R}^3 \times \mathbb{R}^3. \end{aligned} \tag{2}$$

Given the state space (1), its tangent set at a $z \in \mathbb{Z}$ is given by

$$\begin{aligned} T_z\mathbb{Z} = \big\{ &(\delta p, \delta n, \delta p_1, \delta p_2, \delta v, \delta\omega, \delta v_2, \delta v_1) \in (\mathbb{R}^3)^{18} : \\ &\delta n^T n = 0, \delta n^T \omega + n^T \delta\omega = 0, \\ &(p_i - (p + d_i n))^T (\delta p_i - (\delta p + d_i \delta n)) = 0, i \in \{1,2\}, \\ &(\delta v_i - (\delta v + d_i \mathcal{S}(\delta\omega)\, n + d_i \mathcal{S}(\omega)\, \delta n))^T (p_i - (p + d_i n)) + (v_i - (v + d_i \mathcal{S}(\omega)\, n))^T (\delta p_i - (\delta p + d_i \delta n)) = 0 \big\}. \end{aligned}$$

Moreover, the state space definition in (1) allows for the definition of the cables' unit vectors (see Fig. 1) and their angular velocity. Namely, for $i \in \{1,2\}$, we define

$$\mathbb{Z} \ni z \mapsto n_i(z) := \frac{p_i - (p + d_i n)}{\|p_i - (p + d_i n)\|} \overset{(1)}{=} \frac{p_i - (p + d_i n)}{l_i} \in \mathbb{S}^2, \tag{3}$$

$$\mathbb{Z} \ni z \mapsto \omega_i(z) := \mathcal{S}(n_i(z))\, \frac{v_i - (v + d_i \mathcal{S}(\omega)\, n)}{l_i} \in T_{n_i(z)}\mathbb{S}^2, \tag{4}$$

where (3) can be visualized in Fig 1. Given an appropriate $u : \mathbb{R}_{\geq 0} \mapsto \mathbb{R}^6$, a system's trajectory $z : \mathbb{R}_{\geq 0} \ni t \mapsto z(t) \in \mathbb{Z}$ evolves according to

$$\dot{z}(t) = Z(z(t), u(t)), z(0) \in \mathbb{Z}, \tag{5}$$

where $Z : \mathbb{Z} \times \mathbb{R}^6 \ni (z,u) \mapsto Z(z,u) \in \mathbb{R}^{24}$ is given by

$$Z(z,u) := \begin{bmatrix} v \\ \mathcal{S}(\omega)\, n \\ v_1 \\ v_2 \\ \sum_{i\in\{1,2\}} \frac{T_i(z,u)}{m} n_i(z) - g e_3 \\ \sum_{i\in\{1,2\}} \frac{T_i(z,u)}{J} \mathcal{S}(d_i n)\, n_i(z) \\ \frac{u_1}{m_1} - \frac{T_1(z,u)}{m_1} n_1(z) - g e_3 \\ \frac{u_2}{m_2} - \frac{T_2(z,u)}{m_2} n_2(z) - g e_3 \end{bmatrix} \left(= \begin{bmatrix} \dot{p} \\ \dot{n} \\ \dot{p}_1 \\ \dot{p}_2 \\ \dot{v} \\ \dot{\omega} \\ \dot{v}_1 \\ \dot{v}_2 \end{bmatrix} \right), \tag{6}$$

with g as the acceleration due to gravity; and T_1, T_2 as the tensions on the cables (see Fig 1). The linear and angular accelerations in (6) are written from the Newton's and Euler's equations of motion, considering the net force and torque on each rigid body: the bar is taken as a rigid body (with net force and torque in blue – see Fig. 1); while the quadrotors are taken as point masses (with net forces in orange and green – see Fig. 1). The tensions T_1 and T_2 constitute internal forces and the Newton's and Euler's equations of motion do not provide any insight into these forces. However, the constraint that the state must remain in the state set $\mathbb{Z}$ in (1), enforces the vector field Z in (6) to be in the tangent set. This constraint uniquely defines the tensions on the cables, i.e., for any $(z,u) \in \mathbb{Z} \times \mathbb{R}^6$,

$$Z(z,u) \in T_z\mathbb{Z} \Rightarrow \begin{bmatrix} T_1(z,u) \\ T_2(z,u) \end{bmatrix} = M_T^{-1} \left(\begin{bmatrix} \frac{m}{m_1} n_1(z)^T u_1 \\ \frac{m}{m_2} n_2(z)^T u_2 \end{bmatrix} + m \begin{bmatrix} \frac{\|v_1 - (v + d_1 n)\|^2}{l_1} \\ \frac{\|v_2 - (v + d_1 n)\|^2}{l_2} \end{bmatrix} + m\|\omega\|^2 \begin{bmatrix} d_1 n^T n_1(z) \\ d_2 n^T n_2(z) \end{bmatrix} \right), \text{ where} \tag{7}$$

$$M_T \equiv \begin{bmatrix} \frac{m}{m_1} & 0 \\ 0 & \frac{m}{m_2} \end{bmatrix} + \begin{bmatrix} 1 & \cos(\theta) \\ \cos(\theta) & 1 \end{bmatrix} + \frac{m d_1 d_2}{J} \begin{bmatrix} \frac{d_1}{d_2}\|a\|^2 & a^T b \\ a^T b & \frac{d_2}{d_1}\|b\|^2 \end{bmatrix} \Big|_{\substack{\cos(\theta) = n_1(z)^T n_2(z) \\ a = \mathcal{S}(n) n_1(z) \\ b = \mathcal{S}(n) n_2(z)}}.$$

(The matrix M_T in (7) is invertible since it is positive definite, i.e., $M_T > 0$.) The Euler-Lagrange formalism provides an alternative, but equivalent, approach for obtaining the vector field in (6). Finally, note that for

$$\begin{aligned} z^\star &:= (p^\star, n^\star, p_1^\star, p_2^\star, v^\star, \omega^\star, v_1^\star, v_2^\star) \in \mathbb{Z} \\ &:= (0_3, e_1, d_1 e_1 + l_1 e_3, d_2 e_1 + l_2 e_3, 0_3, 0_3, 0_3, 0_3), \end{aligned} \tag{8}$$

and $u^\star := (u_1^\star, u_2^\star) \in \mathbb{R}^6$ as

$$u^\star := \left(\left(m_1 + \frac{m d_2}{d_2 - d_1} \right) g e_3, \left(m_2 + \frac{m d_1}{d_1 - d_2} \right) g e_3 \right), \tag{9}$$

it follows that $Z(z^\star, u^\star) = 0_{24}$, and thus $z^\star$ (under a constant input $u^\star$) constitutes an equilibrium of the system. We can now formulate the problem treated in this paper.

Problem 1: Given the vector field Z in (6) and the equilibrium $z^\star$ in (8), design a control law $u^{cl} : \mathbb{Z} \mapsto \mathbb{R}^6$ satisfying $u^{cl}(z^\star) = u^\star$ and such that $z^\star$ is an exponentially stable equilibrium of $\mathbb{Z} \ni z \mapsto Z(z, u^{cl}(z)) \in T_z\mathbb{Z}$.

Remark 1: In general, we may require the bar to stabilize around any point $p^\star \in \mathbb{R}^3$ and any attitude $n^\star \in \mathbb{S}^2$ with $e_3^T n^\star = 0$. Indeed, that is the case, since, given the automorphism $\phi : \mathbb{Z} \ni z \mapsto \phi(z) \in \mathbb{Z}$ defined as $\phi(z) := (p -$

$p^\star, R^T n, p_1 - (p^\star + d_1 n^\star + l_1 e_3), p_2 - (p^\star + d_2 n^\star + l_2 e_3), v, R^T\omega, v_1, v_2)$ with $R := \begin{bmatrix} n^\star & \mathcal{S}(e_3)\, n^\star & e_3 \end{bmatrix} \in \mathbb{SO}(3)$, it holds that $\mathbb{Z} \times \mathbb{R}^6 \ni (\tilde{z}, u) \mapsto D\phi(z) Z(z,u)|_{z=\phi^{-1}(\tilde{z})} = Z(\tilde{z}, u) \in T_{\tilde{z}}\mathbb{Z}$; that is, the dynamics under the transformation ϕ remain unchanged.

IV. PD Control Law

In this section, we present a PD-like control law, and later, in Section IX, we add an integral term, which adds robustness against disturbances and model uncertainties. For each aerial vehicle $i \in \{1, 2\}$, consider then the control law $u_i^{pd} : \mathbb{Z} \ni z \mapsto u_i^{pd}(z) \in \mathbb{R}^3$ defined as

$$\begin{aligned} u_i^{pd}(z) &:= -\begin{bmatrix} m_i(k_{p,x}\sigma(e_1^T(p_i - p_i^\star), \sigma_{p,x}) + k_{d,x}\sigma(e_1^T(v_i - v_i^\star), \sigma_{d,x})) \\ m_i(k_{p,y}\sigma(e_2^T(p_i - p_i^\star), \sigma_{p,y}) + k_{d,y}\sigma(e_2^T(v_i - v_i^\star), \sigma_{d,y})) \\ \left(m_i + \frac{m}{2}\right)(k_{p,z}\sigma(e_3^T(p_i - p_i^\star), \sigma_{p,z}) + k_{d,z}\sigma(e_3^T(v_i - v_i^\star), \sigma_{d,z})) \end{bmatrix} \\ &\overset{(8)}{=} -\begin{bmatrix} m_i(k_{p,x}\sigma(e_1^T p_i - d_i e_1, \sigma_{p,x}) + k_{d,x}\sigma(e_1^T v_i, \sigma_{d,x})) \\ m_i(k_{p,y}\sigma(e_2^T p_i, \sigma_{p,y}) + k_{d,y}\sigma(e_2^T v_i, \sigma_{d,y})) \\ \left(m_i + \frac{m}{2}\right)(k_{p,z}\sigma(e_3^T p_i - l_i, \sigma_{p,z}) + k_{d,z}\sigma(e_3^T v_i, \sigma_{d,z})) \end{bmatrix}, \end{aligned} \tag{10}$$

where σ is a saturation function (see Notation); $k_{p,k}$ and $k_{d,k}$, for $k \in \{x, y, z\}$, are positive gains related to the position and velocity feedback, respectively; and $\sigma_{p,k}$ and $\sigma_{d,k}$, for $k \in \{x, y, z\}$, are saturations related to the position and velocity feedback, respectively. Note that the control law in (10) is bounded, which is a practical important requirement. The complete control law is then defined as

$$u^{cl} : \mathbb{Z} \ni z \mapsto u^{cl}(z) := u^\star + (u_1^{pd}(z), u_2^{pd}(z)) \in \mathbb{R}^6, \tag{11}$$

and it satisfies $u^{cl}(z^\star) = u^\star$ (see Problem 1 and (9)). In the next Sections, we study the stability of the equilibrium $z^\star$ of the closed loop vector field

$$Z^{cl} : \mathbb{Z} \ni z \mapsto Z^{cl}(z) := Z(z, u^{cl}(z)) \in T_z\mathbb{Z}. \tag{12}$$

V. Routh's Criterion

In Section VII, we linearize the closed loop vector field around the equilibrium, and we verify that the Jacobian is similar to a block triangular matrix, whose block diagonal entries are in controllable form. This section provides immediate tools for the analysis of the eigenvalues of those matrices in controllable form. Denote then, for any $n \in \mathbb{N}$, $C_n : \mathbb{R}^n \ni (a_0, \cdots, a_{n-1}) =: a \mapsto C(a) \in \mathbb{R}^{n\times n}$ defined as

$$C_n(a) := \begin{bmatrix} 0 & 1 & 0 & \cdots & 0 \\ 0 & 0 & 1 & \cdots & 0 \\ \vdots & \vdots & \vdots & \ddots & \vdots \\ 0 & 0 & 0 & \cdots & 1 \\ -a_0 & -a_1 & -a_2 & \cdots & -a_{n-1} \end{bmatrix}, \tag{13}$$

which yields a matrix in a controllable form, and whose eigenvalues are those in $\{\lambda \in \mathbb{C} : \sum_{i=0}^{i=n} a_i \lambda^i = 0\}$. It follows from the Routh's criterion that

$$C_2((a_0, a_1)) \text{ Hurwitz} \Leftrightarrow a_0, a_1 > 0, \tag{14}$$

$$C_3((a_0, a_1, a_2)) \text{ Hurwitz} \Leftrightarrow a_0, a_1, a_2 > 0 \wedge a_0 < a_1 a_2, \tag{15}$$

which we make use of later on. In what follows, denote $p := (p_1, p_2, p_3) \in (\mathbb{R}_{\geq 0})^3, k := (k_p, k_d) \in (\mathbb{R}_{\geq 0})^2$, where, in later sections, p provides physical constants of interest, and k provides the controller gains (in particular a proportional and a derivative gain). There are three matrices (in controllable form) that appear several times in Sections VII–IX, and therefore we introduce them here. Specifically, for $l \in \{3, 4, 5\}$, we define $\Gamma_l : (\mathbb{R}_{\geq 0})^3 \times (\mathbb{R}_{\geq 0})^2 \ni (p, k) \mapsto C_l(p, k) \in \mathbb{R}^{l\times l}$ as

$$\Gamma_3(p, k) := C_3((p_3 k_p + p_3 p_2, p_3 k_d + p_2, p_3)), \tag{16}$$

$$\Gamma_4(p, k) := C_4((p_1 k_p, p_1 k_d, k_p + p_1 + p_2, k_d)) \tag{17}$$

$$\Gamma_5(p, k) := C_5(p_3 e + (p_1 + p_2)(0, 0, 0, 1, 0))|_{e=(p_1 k_p, p_1 k_d, k_p + p_1 + p_2, k_d, 1)}. \tag{18}$$

Since we are interested in determining the stability of an equilibrium, it proves useful to determine when a matrix is Hurwitz. That it is the case iff all the elements in the first column of the Routh's table are positive (or negative). In particular, the

first column of the Routh's tables for the matrices (16)–(18) are, respectively,

$$\begin{bmatrix} 1 & p_3 & \gamma & p_3(p_2+k_p) \end{bmatrix}|_{\gamma=k_dp_3-k_p}, \\ \begin{bmatrix} 1 & k_d & p_2+k_p & \frac{p_1p_2k_d}{p_2+k_p} & p_1k_p \end{bmatrix}, \\ \begin{bmatrix} 1 & p_3 & \gamma & p_3(p_2+k_p) & \frac{p_1p_2}{p_2+k_p}\gamma & p_1p_3k_p \end{bmatrix}|_{\gamma=k_dp_3-k_p}, \tag{19}$$

and thus (17) is Hurwitz for all $(p,k) \in (\mathbb{R}_{\geq 0})^3 \times (\mathbb{R}_{\geq 0})^2$, while (16) and (18) are Hurwitz if and only if

$$p_3 > \frac{k_p}{k_d}. \tag{20}$$

VI. Stability analysis of unit vector dynamics

In Section VII, we look at the kinematics and dynamics of three unit vectors, namely the bar's unit vector and the cables' unit vectors. These unit vectors and corresponding angular velocities are constrained in a manifold of dimension 4 and embedded in a Euclidean space of dimension 6, namely $\mathbb{O} := \{(\nu, \varpi) \in \mathbb{R}^3 \times \mathbb{R}^3 : \nu^T\nu = 1, \nu^T\varpi = 0\}$. For that reason, a linearization of a vector field in $\mathbb{O}$ (and around an equilibrium in $\mathbb{O}$) always yields a Jacobian with two zero eigenvalues, and thus standard linearization theorems cannot be invoked. In this section, we solve this problem by adding to the above vector field an additional vector field that vanishes at the manifold, and thus does not affect solutions; however, this additional vector field replaces the zero eigenvalues by any desired eigenvalues (which we will pick to be real negative).

From now on, we always decompose a $\theta \in \mathbb{O}$ as $\theta \in \mathbb{O} :\Leftrightarrow (\nu, \varpi) \in \mathbb{O}$. A trajectory $\theta : \mathbb{R}_{\geq 0} \ni t \mapsto \theta(t) \in \mathbb{O}$ satisfies $\dot{\theta}(t) = \Theta_1(\theta(t))$ for all $t \geq 0$ and $\theta(0) \in \mathbb{O}$, where the vector field $\Theta_1 : \mathbb{O} \ni \theta \mapsto \Theta_1(\theta) \in T_\theta\mathbb{O}$ is defined as

$$\Theta_1(\theta) := \begin{bmatrix} \mathcal{S}(\varpi)\,\nu \\ \Pi(\nu)\,h(\nu,\varpi) \end{bmatrix},$$

where $h : \mathbb{O} \ni \theta \mapsto h(\nu,\varpi) \in \mathbb{R}^3$ satisfies $h(\nu^\star, 0_3) = 0_3$ for some $\nu^\star \in \mathbb{S}^2$. As such, $\theta^\star := (\nu^\star, 0_3) \in \mathbb{O}$ is an equilibrium since $\Theta_1(\theta^\star) = 0_6$. A linearization procedure yields the Jacobian (see Notation for meaning of $\backsimeq$)

$$D\Theta_1(\theta^\star) = \begin{bmatrix} 0_{3\times3} & -\mathcal{S}(\nu^\star) \\ \Pi(\nu^\star)\,D_1f(e,0_3) & \Pi(\nu^\star)\,D_2f(e,0_3) \end{bmatrix} \backsimeq \begin{bmatrix} \star_{4\times4} & \star_{4\times2} \\ 0_{2\times4} & 0_{2\times2} \end{bmatrix} \tag{21}$$

which has two zero eigenvalues regardless of the choice of h (D_i denotes the derivative w.r.t. the ith argument, for $i \in \{1,2\}$). We solve this problem by introducing an additional vector field, namely $\Theta_2 : \mathbb{R}^3 \times \mathbb{R}^3 \ni (\nu,\varpi) =: \theta \mapsto \Theta_2(\theta) \in \mathbb{R}^3 \times \mathbb{R}^3$ defined as

$$\Theta_2(\theta) := \begin{bmatrix} \Theta_n(\nu) \\ \Theta_\varpi(\nu,\varpi) \end{bmatrix} := \begin{bmatrix} \nu(1-\nu^T\nu) \\ -\nu\nu^T\varpi \end{bmatrix}, \tag{22}$$

where we emphasize that Θ_2 vanishes at $\mathbb{O}$, i.e., that $\Theta_2(\theta) = 0_6, \forall\theta \in \mathbb{O}$; and that the Jacobian of Θ_2 around the equilibrium (and w.r.t. the same similarity matrix as in (21)) is given by

$$D\Theta_2(\theta^\star) = -\begin{bmatrix} \nu^\star\nu^{\star T} & 0_{3\times3} \\ 0_{3\times3} & \nu^\star\nu^{\star T} \end{bmatrix} \simeq 0_{4\times4} \oplus (-I_2).$$

Given any $\lambda > 0$, consider then the new vector field $\Theta_3 : \mathbb{O} \ni \theta \mapsto \Theta_3(\theta) := \Theta_1(\theta) + \lambda\Theta_2(\theta) \in T_\theta\mathbb{O}$, where we emphasize that $\Theta_3(\theta) = \Theta_1(\theta)$ for all $\theta \in \mathbb{O}$. The Jacobian of Θ_3 around the equilibrium then yields

$$D\Theta_3(\theta^\star) = D\Theta_1(\theta^\star) + D\Theta_2(\theta^\star) \backsimeq \begin{bmatrix} 0_{2\times2} & I_2 \\ [0_{2\times1}\ I_2]D_1h(\nu^\star,0_3) & [0_{2\times1}\ I_2]D_2h(\nu^\star,0_3) \end{bmatrix} \oplus (-\lambda I_{2\times2}). \tag{23}$$

For example, for $\mathbb{O} \ni \theta \mapsto h(\nu,\varpi) := -k_d\varpi - k_p\mathcal{S}(e_1)\,\nu \in \mathbb{R}^3$ for some positive k_p and k_d, it follows that (23) reduces to

$$\begin{bmatrix} 0_{3\times3} & I_2 \\ -k_pI_2 & -k_dI_2 \end{bmatrix} \oplus (-\lambda I_{2\times2}),$$

which is Hurwitz. This allows us to conclude that the equilibrium $\theta^\star = (e_1, 0_3)$ is (locally) exponentially stable.

VII. Coordinate transformation to unit vectors and Linearization

In order to apply the results from Section VI, we must perform a simple coordinate transformation. In the new coordinate system, the state space is

$$\mathbb{X} := \big\{\,(p,v,n,\omega,n_1,\omega_1,n_2,\omega_2) \in (\mathbb{R}^3)^8 : (n,\omega) \in \mathbb{O}, (n_1,\omega_1) \in \mathbb{O}, (n_2,\omega_2) \in \mathbb{O}\big\},$$

and, hereafter, given an $x \in \mathbb{X}$, we always decompose it as $x \in \mathbb{X} :\Leftrightarrow (p, v, n, \omega, n_1, \omega_1, n_2, \omega_2) \in \mathbb{X}$. Consider then the coordinate transformations $g_{\mathbb{z}}^{\mathbb{x}} : \mathbb{Z} \ni z \mapsto g_{\mathbb{z}}^{\mathbb{x}}(z) \in \mathbb{X}$ and $g_{\mathbb{x}}^{\mathbb{z}} : \mathbb{X} \ni x \mapsto g_{\mathbb{x}}^{\mathbb{z}}(x) \in \mathbb{Z}$ defined as

$$g_{\mathbb{z}}^{\mathbb{x}}(z) := \begin{bmatrix} p \\ v \\ n \\ \omega \\ n_1(z) \\ \omega_1(z) \\ n_2(z) \\ \omega_2(z) \end{bmatrix} \left(= \begin{bmatrix} p \\ v \\ n \\ \omega \\ n_1 \\ \omega_1 \\ n_2 \\ \omega_2 \end{bmatrix} \right), g_{\mathbb{x}}^{\mathbb{z}}(x) := \begin{bmatrix} p \\ n \\ p + d_1 n + l_1 n_1 \\ p + d_2 n + l_2 n_2 \\ v \\ \mathcal{S}(\omega) n \\ v + d_1 \mathcal{S}(\omega) n + l_1 \mathcal{S}(\omega_1) n_1 \\ v + d_2 \mathcal{S}(\omega) n + l_2 \mathcal{S}(\omega_2) n_2 \end{bmatrix} \left(= \begin{bmatrix} p \\ n \\ p_1 \\ p_2 \\ v \\ \omega \\ v_1 \\ v_2 \end{bmatrix} \right),$$

where it is easy to verify that $g_{\mathbb{x}}^{\mathbb{z}} \circ g_{\mathbb{z}}^{\mathbb{x}} = \mathrm{id}_{\mathbb{Z}}$ and that $g_{\mathbb{z}}^{\mathbb{x}} \circ g_{\mathbb{x}}^{\mathbb{z}} = \mathrm{id}_{\mathbb{X}}$ (the functions n_i and ω_i in $g_{\mathbb{z}}^{\mathbb{x}}$ are those in (3) and (4)). Given a solution $\mathbb{R}_{\geq 0} \ni t \mapsto z(t) \in \mathbb{Z}$ of (5), it then follows that $\mathbb{R}_{\geq 0} \ni t \mapsto x(t) := g_{\mathbb{z}}^{\mathbb{x}}(z(t)) \in \mathbb{X}$ satisfies $\dot{x}(t) = X_1(x(t))$ for all $t \geq 0$ and $x(0) := g_{\mathbb{z}}^{\mathbb{x}}(z(0))$ where

$$X_1 : \mathbb{X} \ni x \mapsto X_1(x) := Dg_{\mathbb{z}}^{\mathbb{x}}(z) Z^{cl}(z)|_{z = g_{\mathbb{x}}^{\mathbb{z}}(x)} \in T_x \mathbb{X},$$

with Z^{cl} as in (12); and where $x^\star := g_{\mathbb{z}}^{\mathbb{x}}(z^\star) \in \mathbb{X}$, with $z^\star$ in (8), is an equilibrium of X_1. Following the reasoning from Section VI, we pick any $\lambda > 0$ and define the vector field $X_3 : \mathbb{X} \ni x \mapsto X_3(x) \in T_x \mathbb{X}$ as

$$X_3(x) := X_1(x) + \lambda X_2(x) := X_1(x) + \lambda \begin{bmatrix} 0_6 \\ \Theta_2((n, \omega)) \\ \Theta_2((n_1, \omega_1)) \\ \Theta_2((n_2, \omega_2)) \end{bmatrix} = \left(\begin{bmatrix} (\dot{p}, \dot{v}) \\ (\dot{n}, \dot{\omega}) \\ (\dot{n}_1, \dot{\omega}_1) \\ (\dot{n}_2, \dot{\omega}_2) \end{bmatrix} \right), \tag{24}$$

with Θ_2 as in (22). Linearization around $x^\star$ yields the Jacobian

$$A = DX_3(x^\star) \in \mathbb{R}^{24 \times 24}, \tag{25}$$

which is not a diagonal matrix, and thus determining whether it is Hurwitz is not straightforward. For that purpose, we provide a similarity matrix, called $P \in \mathbb{R}^{24 \times 24}$, such that PAP^{-1} is a block triangular matrix, and where each block diagonal matrix is in controllable form (allowing us to invoke the results from Section V). Later, we also provide a physical interpretation for the similarity transformation P.

Assumption 2: Hereafter, we assume that $m_1 = m_2 =: M$, that $l_1 = l_2 =: l$, and that $d_1 = -d_2 =: d$. Without these assumptions, the Jacobian in (25) is still equivalent to a block triangular matrix, but the block diagonal elements are larger in dimension when compared to those in (27). Analysis for the general case is left for future research. Nonetheless, the experiments in Section X indicate robustness of the results that follow against model mismatches, where these assumptions are not exactly met.

Consider then the similarity matrix

$$P := \begin{bmatrix} P_z & P_\theta & P_x & P_\delta & P_y & P_\psi & P_\perp \end{bmatrix}^T \in \mathbb{R}^{24 \times 24}, \tag{26}$$

where (below A is the Jacobian in (25))

$$\begin{aligned}
P_z &:= \begin{bmatrix} e_3 & Ae_3 \end{bmatrix} \in \mathbb{R}^{24 \times 2}, P_\theta := \begin{bmatrix} e_9 & Ae_9 \end{bmatrix} \in \mathbb{R}^{24 \times 2}, \\
P_x &:= \begin{bmatrix} e_1 & Ae_1 & A^2 e_1 & A^3 e_1 \end{bmatrix} \in \mathbb{R}^{24 \times 4}, \\
P_\delta &:= \begin{bmatrix} (e_{13} - e_{19}) & A(e_{13} - e_{19}) \end{bmatrix} \in \mathbb{R}^{24 \times 2}, \\
P_y &:= \begin{bmatrix} e_2 & Ae_2 & A^2 e_2 & A^3 e_2 \end{bmatrix} \in \mathbb{R}^{24 \times 4}, \\
P_\psi &:= \begin{bmatrix} e_8 & Ae_8 & A^2 e_8 & A^3 e_8 \end{bmatrix} \in \mathbb{R}^{24 \times 4}, \\
P_\perp &:= \begin{bmatrix} e_7 & e_{10} & e_{15} & e_{18} & e_{21} & e_{24} \end{bmatrix} \in \mathbb{R}^{24 \times 6}.
\end{aligned}$$

Remark 3: Given the decomposition $x \in \mathbb{X} :\Leftrightarrow (p, v, n, \omega, n_1, \omega_1, n_2, \omega_2) \in \mathbb{X}$, and since for the linearized motion $\dot{x} = Ax$, it follows from the similarity matrix P in (26) that

$$P^T x = \begin{bmatrix} P_z^T x \\ P_\theta^T x \\ P_x^T x \\ P_\delta^T x \\ P_y^T x \\ P_\psi^T x \end{bmatrix} = \begin{bmatrix} (e_3^T p^{(0)}, e_3^T p^{(1)}) \\ (e_3^T n^{(1)}, e_3^T n^{(1)}) \\ (e_1^T p^{(0)}, e_1^T p^{(1)}, e_1^T p^{(2)}, e_1^T p^{(3)}) \\ (e_1^T (n_1^{(0)} - n_2^{(0)}), e_1^T (n_1^{(1)} - n_2^{(1)})) \\ (e_2^T p^{(0)}, e_2^T p^{(1)}, e_2^T p^{(2)}, e_2^T p^{(3)}) \\ (e_2^T n^{(0)}, e_2^T n^{(1)}, e_2^T n^{(2)}, e_2^T n^{(3)}) \end{bmatrix} = \begin{bmatrix} z \text{ linear motion of bar (2nd order)} \\ z \text{ angular motion of bar (2nd order)} \\ x \text{ linear motion of bar (4th order)} \\ x \text{ difference motion between cables (2nd order)} \\ y \text{ linear motion of bar (4th order)} \\ y \text{ angular motion of bar (4th order)} \end{bmatrix},$$

which provides an intuition for the meaning of the similarity matrix P.
Given the state matrix A in (25) and the similarity matrix P in (26), it then follows that

$$A \simeq PAP^{-1} = \begin{bmatrix} A_z \oplus A_\theta \oplus A_x \oplus A_\delta \oplus A_y \oplus A_\psi & \star \\ 0_{6\times 18} & -\lambda I_{6\times 6} \end{bmatrix}, \tag{27}$$

where (27) is a block triangular matrix, with the first block as a block diagonal matrix. Thus $\text{eig}(A) = \{-\lambda\} \cup \text{eig}(A_z) \cup \cdots \cup \text{eig}(A_\psi)$, and, therefore, determining whether the Jacobian A in (25) is Hurwitz amounts to checking whether each block diagonal matrix in (27) is Hurwitz. Recalling the definitions in Section V, namely (13) and (16)–(18), the matrices in (27) are given by

$$A_z = C_2((k_{p,z}, k_{d,z})), \tag{28}$$

$$A_\theta = C_2\left(\frac{d^2(2M+m)}{J+2d^2M}(k_{p,z}, k_{d,z})\right), \tag{29}$$

and

$$A_x = \Gamma_4(p,k)\,|_{p=(\frac{g}{l}, \frac{g}{l}\frac{m}{2M}, 0), k=(k_{p,x}, k_{d,x})}, \tag{30}$$

$$A_\delta = C_2\left(\left(k_{p,x} + \frac{g}{L}\frac{m}{2M}, k_{d,z}\right)\right), \tag{31}$$

and

$$A_y = \Gamma_4(p,k)\,|_{p=(\frac{g}{l}, \frac{g}{l}\frac{m}{2M}, 0), k=(k_{p,y}, k_{d,y})}, \tag{32}$$

$$A_\psi = \Gamma_4(p,k)\,|_{p=(\frac{g}{l}\frac{d^2m}{J}, \frac{g}{l}\frac{m}{2M}, 0), k=(k_{p,y}, k_{d,y})}. \tag{33}$$

It thus follows from (14) and (19) that A in (25) is Hurwitz, since all matrices in (27) are Hurwitz.

Let us now provide some intuition into the meaning of the similarity matrix P and the matrices in (27). Recall the decomposition of the state z in (2). Since $P_z z = e_3^T p =: p_z$ and $P_\theta z = e_3^T n =: \theta$, it follows from (28) and (29) that, for the linearized motion, the bar's z-position and the bar's z-attitude behave as second-order integrators, i.e.,

$$p_z^{(2)}(t) = (A_z)_{2,2} p_z^{(1)}(t) + (A_z)_{2,1} p_z^{(0)}(t),$$
$$\theta^{(2)}(t) = (A_\theta)_{2,2}\theta^{(1)}(t) + (A_x)_{2,1}\theta^{(0)}(t).$$

Since $P_x z = e_1^T p =: p_x$ and $P_\delta z = e_1^T(n_1 - n_2) =: \delta$, it follows from (30) and (31) that, for the linearized motion, the bar's x-position behaves as a fourth-order integrator and the cables' unit vectors displacement from each other in the x-direction behaves as a second-order integrator, i.e.,

$$p_x^{(4)}(t) = (A_x)_{4,4} p_x^{(3)}(t) + \cdots + (A_x)_{4,1} p_x^{(0)}(t),$$
$$\delta^{(2)}(t) = (A_\delta)_{2,2}\delta^{(1)}(t) + (A_\delta)_{2,1}\delta^{(0)}(t).$$

Finally, since $P_y z = e_2^T p =: p_y$ and $P_\psi z = e_2^T n =: \psi$, it follows from (32) and (33) that, for the linearized motion, the bar's y-position and the bar's y-attitude behave as fourth-order integrators, i.e.,

$$p_y^{(4)}(t) = (A_y)_{4,4} p_y^{(3)}(t) + \cdots + (A_y)_{4,1} p_y^{(0)}(t),$$
$$\psi^{(4)}(t) = (A_\psi)_{4,4}\psi^{(3)}(t) + \cdots + (A_x)_{4,1}\psi^{(0)}(t).$$

Finally, $P_\perp$ collects all the components along which the eigenvalues would be zero if not for the contribution of the extra term in (24). Finally, we also emphasize that, for the linearized motion, and for $i \in \{x, y, z\}$, the proportional and derivative gains $k_{p,i}$ and $k_{d,i}$ have an effect on the i-motion only, which agrees with intuition.

VIII. Attitude Control Inner Loop

Previously, in Section III, we assumed that the quadrotrors provide a three dimensional force without delay. However, that is not the case in a real aerial vehicle, where there is an internal attitude inner loop, and it is important to study the effect of that inner loop in the closed loop stability for the proposed control law in (11). In this section, we work with an augmented state, namely

$$\bar{z} = (z, r_1, r_2) \in \mathbb{Z} \times \mathbb{S}^2 \times \mathbb{S}^2 =: \bar{\mathbb{Z}} \tag{34}$$

where $r_1, r_2 \in \mathbb{S}^2$ stand for the quadrotor's direction where input thrust is provided (see Fig. 1), and with z as in (2). The state $\bar{z} : \mathbb{R}_{\geq 0} \ni t \mapsto \bar{z}(t) \in \bar{\mathbb{Z}}$ evolves according to

$$\dot{\bar{z}}(t) = \bar{Z}(\bar{z}(t), u(t)), \bar{z}(0) \in \bar{\mathbb{Z}},$$

where $\bar{Z}:\bar{\mathbb{Z}}\times(\mathbb{R}^3\backslash\{0_3\})^2\ni(\bar{z},u)\mapsto\bar{Z}(\bar{z},u)\in T_{\bar{z}}\bar{\mathbb{Z}}$ is given by

$$\bar{Z}(\bar{z},u):=\begin{bmatrix}Z(z,(u_1^Tr_1r_1,u_2^Tr_2r_2))\\ \mathcal{S}\left(\omega_r(r_1,u_1)\right)r_1\\ \mathcal{S}\left(\omega_r(r_2,u_2)\right)r_2\end{bmatrix}\left(=\begin{bmatrix}\dot{z}\\ \dot{r}_1\\ \dot{r}_2\end{bmatrix}\right), \tag{35}$$

$$\omega_r(r_i,u_i):=k_{\bar{\theta}}\mathcal{S}\left(r_i\right)\frac{u_i}{\|u_i\|}, \tag{36}$$

with Z as the vector field in (6); with ω_r as the angular velocity that the attitude inner loop imposes on the vehicle in order to track the desired attitude (namely the direction of the input); and with $k_{\bar{\theta}}$ as the positive gain of the attitude inner loop, where $\frac{1}{k_{\bar{\theta}}}$ may be interpreted as a time constant of a first order system.

The intuition for (36) is simple: for a constant $u\in\mathbb{R}^3$, a solution $t\mapsto r(t)\in\mathbb{S}^2$ of $\dot{r}(t)=\mathcal{S}\left(\omega(r(t),u)\right)r(t)$ converges exponentially fast to $\frac{u}{\|u\|}$, with rate proportional to $k_{\bar{\theta}}$ (and provided that $r(0)\neq-\frac{u}{\|u\|}$). Note that the model for the attitude inner loop of the quadrotors in (35) is only a possible one, and there are more ways of modeling that inner loop. Finally, note that for $\bar{z}^\star:=(z^\star,e_3,e_3)\in\bar{\mathbb{Z}}$, it follows that $\bar{Z}(\bar{z}^\star,u^\star)=0_{30}$ (with $z^\star$ in (8)).

As done in Section VII, we work in a new coordinate system, focused on unit vectors. For that reason, denote $\bar{x}=(x,r_1,r_2)\in\mathbb{X}\times\mathbb{S}^2\times\mathbb{S}^2=:\bar{\mathbb{X}}$, and consider the mappings $g_{\bar{\mathbb{X}}}^{\bar{\mathbb{Z}}}:\bar{\mathbb{X}}\ni\bar{x}\mapsto g_{\bar{\mathbb{X}}}^{\bar{\mathbb{Z}}}(\bar{x}):=(g_{\mathbb{X}}^{\mathbb{Z}}(x),r_1,r_2)\in\bar{\mathbb{Z}}$ and $g_{\bar{\mathbb{Z}}}^{\bar{\mathbb{X}}}:\bar{\mathbb{Z}}\ni\bar{z}\mapsto g_{\bar{\mathbb{Z}}}^{\bar{\mathbb{X}}}(\bar{z}):=(g_{\mathbb{Z}}^{\mathbb{X}}(z),r_1,r_2)\in\bar{\mathbb{X}}$. The control law is still that in (11), and, as in Section VII, we define the vector field

$$\bar{X}_1:\bar{\mathbb{X}}\ni\bar{x}\mapsto\bar{X}_1(\bar{x}):=Dg_{\bar{\mathbb{Z}}}^{\bar{\mathbb{X}}}(\bar{z})\bar{Z}(\bar{z},u_{cl}(z))|_{\bar{z}=g_{\bar{\mathbb{X}}}^{\bar{\mathbb{Z}}}(\bar{x})},$$

and add the extra terms to the latter vector field, i.e., we define $\bar{X}_3:\bar{\mathbb{X}}\ni\bar{x}\mapsto\bar{X}_3(\bar{x})\in T_{\bar{x}}\bar{\mathbb{X}}$ as

$$\bar{X}_3(\bar{x}):=\bar{X}_1(\bar{x})+\lambda\bar{X}_2(\bar{x}):=\bar{X}_1(x)+\lambda\begin{bmatrix}X_2(x)\\ \Theta_n(r_1)\\ \Theta_n(r_2)\end{bmatrix}, \tag{37}$$

with X_2 as in (24) and Θ_n as in (22). Linearization of $\bar{X}_3$ around $\bar{x}^\star:=g_{\bar{\mathbb{Z}}}^{\bar{\mathbb{X}}}(\bar{z}^\star)$, yields the Jacobian $\bar{A}=D\bar{X}_3(\bar{x}^\star)\in\mathbb{R}^{30\times30}$ where

$$\bar{A}\simeq\begin{bmatrix}\bar{A}_z\oplus\bar{A}_\theta\oplus\bar{A}_x\oplus\bar{A}_\delta\oplus\bar{A}_y\oplus\bar{A}_\psi & \star\\ 0_{8\times22} & -\lambda I_{8\times8}\end{bmatrix}, \tag{38}$$

with $\bar{A}_z=A_z\in\mathbb{R}^{2\times2}$ and $\bar{A}_\theta=A_\theta\in\mathbb{R}^{2\times2}$ (see (28) and (29)), and with (recall (16) and (18) from Section V)

$$\bar{A}_x=\Gamma_5\left(p,k\right)|_{p=(\frac{g}{l},\frac{g}{l}\frac{m}{2M},k_{\bar{\theta}}),k=(k_{p,x},k_{d,x})}, \tag{39}$$

$$\bar{A}_\delta=\Gamma_3\left(p,k\right)|_{p=(\frac{g}{l},\frac{g}{l}\frac{m}{2M},k_{\bar{\theta}}),k=(k_{p,x},k_{d,x})},$$

$$\bar{A}_y=\Gamma_5\left(p,k\right)|_{p=(\frac{g}{l},\frac{g}{l}\frac{m}{2M},k_{\bar{\theta}}),k=(k_{p,y},k_{d,y})},$$

$$\bar{A}_\psi=\Gamma_5\left(p,k\right)|_{p=(\frac{g}{l}\frac{d^2m}{J},\frac{g}{l}\frac{m}{2M},k_{\bar{\theta}}),k=(k_{p,y},k_{d,y})}. \tag{40}$$

As concluded in Section V (see (20)), the matrices in (39)-(40) are Hurwitz if and only if

$$k_{\bar{\theta}}>\max\left(\frac{k_{p,x}}{k_{d,x}},\frac{k_{p,y}}{k_{d,y}}\right). \tag{41}$$

The same conclusion extends to the Jacobian $\bar{A}$ owing to (38). Since, we do not have control over $k_{\bar{\theta}}$, preserving stability amounts to guaranteeing that $\frac{k_{p,h}}{k_{d,h}}$, for $h\in\{x,y\}$, remains *small enough*. Intuitively, this implies that *fast* x and y (position and attitude) motions require a *fast* attitude inner loop.

IX. Integral Action

In this section, we provide an integral action mechanism which provides robustness again disturbances and model uncertainties, as shall be verified in the experiments.

From here on, we work with augmented states, specifically

$$\tilde{z}=(\bar{z},\xi_1,\xi_2)\in\bar{\mathbb{Z}}\times\mathbb{R}\times\mathbb{R}=:\tilde{\mathbb{Z}},$$

with $\bar{z}$ as in (34). The state $\tilde{z}:\mathbb{R}_{\geq0}\ni t\mapsto\tilde{z}(t)\in\tilde{\mathbb{Z}}$ evolves according to $\dot{\tilde{z}}(t)=\tilde{Z}(\tilde{z}(t),u(t))$ with $\tilde{z}(0)\in\tilde{\mathbb{Z}}$ and where $\tilde{Z}:\tilde{\mathbb{Z}}\times(\mathbb{R}^3\backslash\{0_3\})^2\ni(\tilde{z},u)\mapsto\tilde{Z}(\tilde{z},u)\in T_{\tilde{z}}\tilde{\mathbb{Z}}$ is given by

$$\tilde{Z}(\tilde{z},u):=\begin{bmatrix}\bar{Z}(z,u)\\ e_3^T(p_1-p_1^\star)\\ e_3^T(p_2-p_2^\star)\end{bmatrix}\overset{(8)}{=}\begin{bmatrix}\bar{Z}(z,u)\\ e_3^Tp_1-l_1\\ e_3^Tp_2-l_2\end{bmatrix}\left(=\begin{bmatrix}\dot{\bar{z}}\\ \dot{\xi}_1\\ \dot{\xi}_2\end{bmatrix}\right), \tag{42}$$

with $\bar{Z}$ as in (35). Thus, physically, ξ_1 and ξ_2 represent the z-position integral error of quadrotor 1 and 2. We emphasize that $\tilde{z}^\star = (\bar{z}^\star, 0_2) \in \tilde{Z}$ is an equilibrium of (42) ($\tilde{Z}(\tilde{z}^\star, u^\star) = 0_{32}$).

Consider then the PID-like control law $\tilde{u}^{cl} : \tilde{\mathbb{Z}} \ni \tilde{z} \mapsto \tilde{u}^{cl}(\tilde{z}) \in \mathbb{R}^6$, based on (11), and defined as

$$\tilde{u}^{cl}(\tilde{z}) := u^{cl}(z) + \begin{bmatrix} (m_1 + \frac{m}{2}) e_3 \sigma(k_{i,z}\xi_1, \sigma_{i,z}) \\ (m_2 + \frac{m}{2}) e_3 \sigma(k_{i,z}\xi_2, \sigma_{i,z}) \end{bmatrix}, \tag{43}$$

where $k_{i,z}$ and $\sigma_{i,z}$ are positive constants related to the integral action gain and the integral action saturation. Following similar steps as in the previous section (and after defining obvious maps $g^{\tilde{\chi}}_{\tilde{z}}$ and $g^{\tilde{z}}_{\tilde{\chi}}$), we define two vectors fields, namely

$$\tilde{X}_1 : \tilde{\mathbb{X}} \ni \tilde{x} \mapsto \tilde{X}_1(\tilde{x}) := Dg^{\tilde{\chi}}_{\tilde{z}}(\tilde{z}) \tilde{Z}(\tilde{z}, \tilde{u}^{cl}(\tilde{z}))|_{\tilde{z}=g^{\tilde{z}}_{\tilde{\chi}}(\bar{x})} \in T_{\tilde{x}}\tilde{\mathbb{X}},$$
$$\tilde{X}_3 : \tilde{\mathbb{X}} \ni \tilde{x} \mapsto \tilde{X}_3(\tilde{x}) := \tilde{X}_1(\tilde{x}) + \lambda(\bar{X}_2(\bar{x}), 0_2) \in T_{\tilde{x}}\tilde{\mathbb{X}},$$

with $\bar{X}_2$ as in (37). Linearization of $\tilde{X}_3$ around the equilibrium $\tilde{x}^\star := g^{\tilde{\chi}}_{\tilde{z}}(\tilde{z}^\star)$ yields the Jacobian

$$\tilde{A} = D\tilde{X}_3(\tilde{x}^\star) \in \mathbb{R}^{32\times 32},$$

where

$$\tilde{A} \simeq \begin{bmatrix} \tilde{A}_z \oplus \tilde{A}_\theta \oplus \tilde{A}_x \oplus \tilde{A}_\delta \oplus \tilde{A}_y \oplus \tilde{A}_\psi & \star \\ 0_{8\times 24} & -\lambda I_{8\times 8} \end{bmatrix}, \tag{44}$$

and with $\tilde{A}_k = \bar{A}_k$ for $k \in \{x, \theta, y, \psi\}$, while

$$\tilde{A}_z = C_3\left((k_{i,z}, k_{p,z}, k_{d,z})\right) \in \mathbb{R}^{3\times 3},$$
$$\tilde{A}_\theta = C_3\left(\frac{d^2(2M+m)}{J+2d^2M}(k_{i,z}, k_{p,z}, k_{d,z})\right) \in \mathbb{R}^{3\times 3}. \tag{45}$$

From (15), $\tilde{A}_z$ and $\tilde{A}_\theta$ are Hurwitz if and only if

$$k_{i,z} < \min\left(1, 1 + \frac{md^2 - J}{2Md^2 + J}\right) k_{p,z}k_{d,z}. \tag{46}$$

Intuitively, (46) requires the integral gain to be *small enough*. Also notice that if d is arbitrarily small, then $k_{i,z}$ needs also be arbitrarily small; this is motivated by (45), and it agrees with intuition, which suggests that controlling the z-attitude motion of the bar becomes difficult if the contact points on the bar are *too close* to its center of mass (see Fig. 1).

For completeness, the similarity matrix in (44) has components $\tilde{P}_z$ and $\tilde{P}_\theta$ which are given by

$$\tilde{P}_z := \begin{bmatrix} e_{31} + e_{32} & \tilde{A}(e_{31} + e_{32}) & \tilde{A}^2(e_{31} + e_{32}) \end{bmatrix} \in \mathbb{R}^{32\times 3},$$
$$\tilde{P}_\theta := \begin{bmatrix} e_{31} - e_{32} & \tilde{A}(e_{31} - e_{32}) & \tilde{A}^2(e_{31} - e_{32}) \end{bmatrix} \in \mathbb{R}^{32\times 3}.$$

Notice that $e_1^T\tilde{P}_z\tilde{z} = \xi_1 + \xi_2$ and that $e_2^T\tilde{P}_z\tilde{z} =: 2e_3^Tp =: 2p_z$, while $e_1^T\tilde{P}_\theta\tilde{z} = \xi_1 - \xi_2$ and $e_2^T\tilde{P}_\theta\tilde{z} = -2de_3^Tn =: -2d\theta$; i.e., the sum of the integral errors is related to the z-position of the bar, while the difference between the integral errors is related to the z-attitude of the bar. In fact, for the linearized motion, $p_z^{(2)}(t) = (\tilde{A}_z)_{3,3}p_z^{(1)}(t) + (\tilde{A}_z)_{3,2}p_z^{(0)}(t) + (\tilde{A}_z)_{3,1}\int_0^t p_z^{(0)}(\tau)d\tau$, and $\theta_z^{(2)}(t) = (\tilde{A}_\theta)_{3,3}\theta^{(1)}(t) + (\tilde{A}_\theta)_{3,2}\theta^{(0)}(t) + (\tilde{A}_\theta)_{3,1}\int_0^t \theta^{(0)}(\tau)d\tau$.

Theorem 4: Consider the quadrotors-bar system with the open loop vector field (42), and the control law (43). Then, the equilibrium $\tilde{z}^\star := (\bar{z}^\star, 0_2) \in \tilde{\mathbb{Z}}$ of $\tilde{\mathbb{Z}} \ni \tilde{z} \mapsto \tilde{Z}(\tilde{z}, \tilde{u}^{cl}(\tilde{z}))$ is exponentially stable if and only if (41) and (46) are satisfied.

Proof: The Jacobian in (44) is Hurwitz iff (41) and (46) are satisfied. Then exponential stability of $\tilde{x}^\star$ for the nonlinear vector field $\tilde{X}_3$ is guaranteed, and exponential stability of $\tilde{z}^\star$ for the nonlinear vector field $\tilde{\mathbb{Z}} \ni \tilde{z} \mapsto \tilde{Z}(\tilde{z}, \tilde{u}^{cl}(\tilde{z}))$ is also guaranteed. ■

One of the motivations for adding integral errors to the control law is to guarantee robustness against model uncertainties. In the next theorem, we assume that the control law in (43) is implemented with $m = 0$ (which is a reasonable assumption, if the aerial vehicles pick an unknown bar), and we guarantee that there exists an exponentially stable equilibrium that still guarantees that Problem 1 is solved (we emphasize that this theorem can be extended to the case where the control law (43) is implemented with a wrong bar mass, rather than assuming that the bar mass is zero).

Theorem 5: Consider the quadrotors-bar system with the open loop vector field (42), and assume the control law (43) is implemented with $m = 0$ and $\sigma_{i,z} > g\frac{m}{2M}$. Then, the equilibrium (for brevity, denote $\gamma := \sigma^{-1}\left(g\frac{m}{2M}, \sigma_{i,z}\right) \in \mathbb{R}$)

$$\tilde{z}^\star := (\bar{z}^\star, \gamma/k_{i,z}, \gamma/k_{i,z}) \in \tilde{\mathbb{Z}}$$

of $\tilde{\mathbb{Z}} \ni \tilde{z} \mapsto \tilde{Z}(\tilde{z}, \tilde{u}^{cl}(\tilde{z}))$ is exponentially stable if and only if (41) and

$$k_{i,z}\sigma'(\gamma, \sigma_{i,z}) < \min\left(\frac{2M}{2M+m}, \frac{2d^2M}{J+2d^2M}\right) k_{p,z}k_{d,z}$$

are satisfied.

Proof: The Jacobian matrix with the control law (43) implemented with $m = 0$ is similar to that in (44), with the only difference that

$$\tilde{A}_z = C_3\left(\frac{2M}{2M+m}(k_{i,z}\sigma'(\gamma,\sigma_{i,z}),k_{p,z},k_{d,z})\right)$$
$$\tilde{A}_\theta = C_3\left(\frac{2d^2M}{J+2d^2M}(k_{i,z}\sigma'(\gamma,\sigma_{i,z}),k_{p,z},k_{d,z})\right).$$

The theorem's conclusion then follow from (15). ■

Theorem 5 is valid for any smooth σ function, but for σ function used (see notation), $\sup_{x\in\mathbb{R}}\sigma'(x,\bar{\sigma}) \leq 1$, which simplifies the results in the theorem.

X. Experimental Results

A video of the experiment that is described in the sequel is found at https://youtu.be/ywwPvZuVpF0, whose results can be visualized in Fig. 2. For the experiment, two commercial quadrotors were used, namely two IRISes+ from 3D Robotics, weighting $M = 1.442$ kg, with a maximum payload of 0.4 kg. The bar was made out of a core of aluminum (to add rigidity to the bar), and surrounded with PVC pipe (to add weight to the bar), and it weighted $m = 0.33$ kg (corresponding to $\approx 23\%$ of each UAV's weight). The bar had a length of 2m, and it was attached to the UAVs by two cables of equal length, specifically $l = l_1 = l_2 = 1.4$ m; the contact points between the bar and the cables were at the extremities of the bar, and thus $d = d_1 = -d_2 = 1$ m. The commands for controlling the quadrotors were processed on a ground station, developed in a ROS environment, and sent to the on-board autopilot, which allowed for remotely controlling the aerial vehicles through a desired three dimensional force input. A wireless radio communication between ground station and autopilot was established through a telemetry radio, using a MAVLink protocol that directly overrode the signals sent from the radio transmitter. The quadrotors' and bar's positions, velocities and orientations were estimated by 12 cameras from a Qualisys motion capture system.

The control law (43) was applied with $m = 0$kg; with $k_{i,z} = 0.5\text{s}^{-3}$ and $\sigma_{i,z} = 5\text{ms}^{-2}$; with $k_{p,x} = k_{p,y} = 2.9\text{s}^{-2}$, $k_{d,x} = k_{d,y} = 2.4\text{s}^{-1}$, $\sigma_{p,x} = \sigma_{p,y} = 1.0$m and $\sigma_{d,x} = \sigma_{d,y} = 1.0\text{ms}^{-1}$; and with $k_{p,z} = 1.0\text{s}^{-2}$, $k_{d,z} = 1.2\text{s}^{-1}$, $\sigma_{p,z} = 0.5$m and $\sigma_{d,z} = 0.5\text{ms}^{-1}$ (see (11)).

In the beginning of the experiment the system quadrotors-bar is required to stabilize around $z^\star$ where $p^\star = 0.4e_3$m and $n^\star = e_2$ (see Remark 1 and see (8)), i.e, the bar is required to hover at 0.4m and required to be aligned with the y-axis. In Fig. 2(d), the bar attitude is parameterized with a pitch and yaw angle, i.e., $n = (\cos(\theta)\cos(\psi), \cos(\theta), \sin(\theta)) \in \mathbb{S}^2$, and, as can be seen in Fig. 2(d) the bar is initially aligned with the y-axis ($\psi = 90^\circ$). At around 60 sec, the bar is required to remain in the same position but to align its orientation with the x-axis ($n^\star = e_1 :\Leftrightarrow \psi^\star = 0^\circ$), which can be seen in Figs. 2(d) and 2(a). At around 70 sec, the bar is required to move 1m in the y-direction ($p^\star = (0, 1, 0.5)m$) while keeping the same orientation ($n^\star = e_1 :\Leftrightarrow \psi^\star = 0^\circ$), which can again be seen in Figs. 2(d) and 2(a). During the same experiment, we also tested robustness against impulse disturbances, which illustrate the size of the basin of attraction of the equilibrium. First, at around 90s, we disturbed the bar position in the y-direction, as can be seen in Fig. 2(a); and, at around 100s, we disturbed the uav 1 position in the y-direction, as can be seen in Fig. 2(b). In both cases, the system quadrotors-bar returns to its equilibrium point.

In Fig. 2(c), the control inputs computed from the control law (43) are shown, which are converted into PWM signals: one for the pitch, one for the roll, and another for the throttle (in this paper, we ignored the yaw motion, and requested the uavs to always keep the same yaw position). The pitch and roll PWM signals have neutral values for which the quadrotors do not pitch nor roll, regardless of battery level; while the throttle PWM signal results in a propulsive power which decays as the battery drains. In Fig 2(f), the integral states, described in Section IX, are shown. There is a trend, where the integral term grows larger while the experiments are running, which stems from the fact that, as the batteries drain, a larger throttle PWM signal needs to be requested from the IRISes+.

XI. Conclusions

We proposed a control law for stabilization of a quadrotors-bar system, and provided conditions on the control law's gains that guarantee exponential stability of the equilibrium. The system was modeled assuming that the UAVs have an attitude inner loop, and a lower bound on the attitude gain, for which exponential stability of the equilibrium is preserved, was provided. An integral action term, to compensate for battery drainage or model mismatches such as an unknown bar mass, was also included, and a bound on the integral gain was provided that guarantees exponential stability is preserved. An experiment demonstrates the system quadrotors-bar stabilizing around different equilibrium points, and it also illustrates the robustness of the proposed control law to impulsive disturbances.

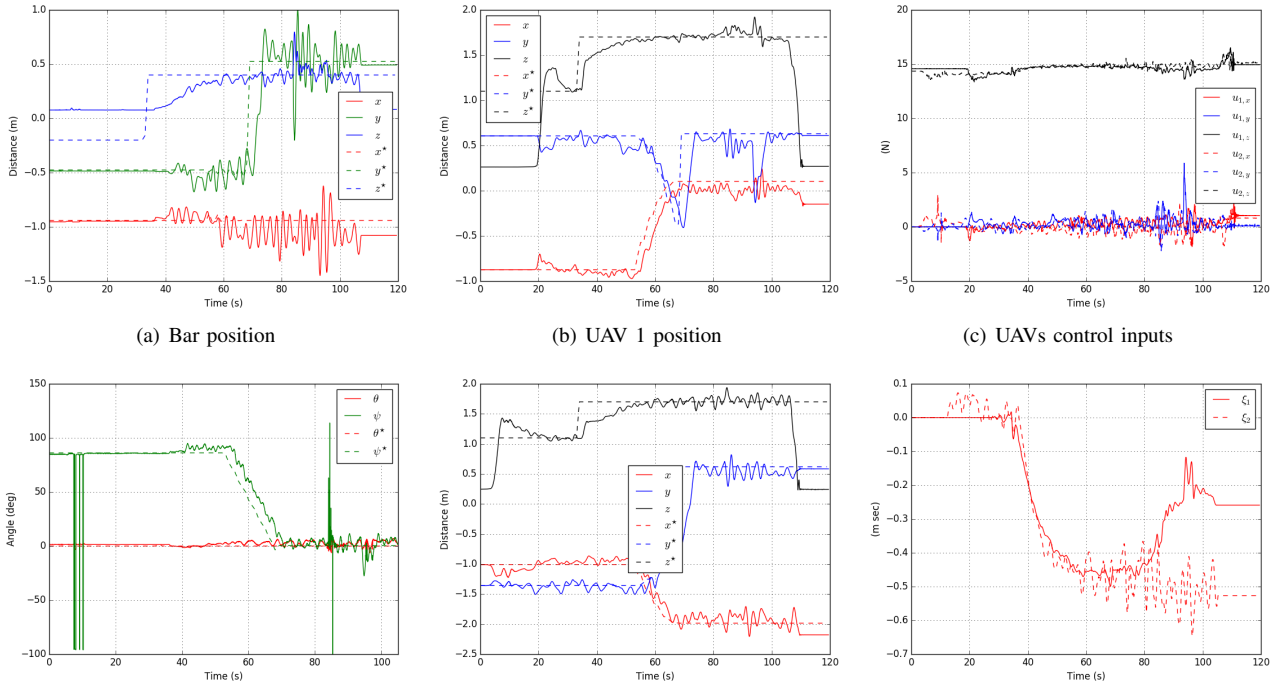

(a) Bar position (b) UAV 1 position (c) UAVs control inputs

(d) Bar orientation (ill-estimated for some time instants) (e) UAV 2 position (f) UAVs integral state

Fig. 2: Experimental results for collaborative bar lifting.

REFERENCES

[1] AEROWORKS aim. http://www.aeroworks2020.eu/.

[2] R. Mahony, V. Kumar, and P. Corke. Multirotor aerial vehicles: Modeling, estimation, and control of quadrotor. *Robotics Automation Magazine, IEEE*, 19(3):20–32, Sept 2012.

[3] M. Hua, T. Hamel, P. Morin, and C. Samson. Introduction to feedback control of underactuated VTOL vehicles: A review of basic control design ideas and principles. *Control Systems*, 33(1):61–75, 2013.

[4] D. Scaramuzza and et al. Vision-controlled micro flying robots: From system design to autonomous navigation and mapping in GPS-denied environments. *Robotics Automation Magazine, IEEE*, 21(3):26–40, Sept 2014.

[5] F. Ruggiero, M.A. Trujillo, R. Cano, H. Ascorbe, A. Viguria, C. Peréz, V. Lippiello, A. Ollero, and B. Siciliano. A multilayer control for multirotor UAVs equipped with a servo robot arm. In *IEEE ICRA*, pages 4014–4020, 2015.

[6] N. Sydney, B. Smyth, and D. A. Paley. Dynamic control of autonomous quadrotor flight in an estimated wind field. In *52nd IEEE Conference on Decision and Control*, pages 3609–3616, Dec 2013.

[7] M. Bernard and K. Kondak. Generic slung load transportation system using small size helicopters. In *IEEE ICRA*, pages 3258–3264. IEEE, 2009.

[8] M. E. Guerrero, D. A. Mercado, R. Lozano, and C. D. García. Passivity based control for a quadrotor UAV transporting a cable-suspended payload with minimum swing. In *2015 54th IEEE Conference on Decision and Control (CDC)*, pages 6718–6723, Dec 2015.

[9] É. Servais, H. Mounier, and B. d'Andréa Novel. Trajectory tracking of trirotor UAV with pendulum load. In *20th International Conference on Methods and Models in Automation and Robotics (MMAR)*, pages 517–522, Aug 2015.

[10] K. Sreenath, N. Michael, and V. Kumar. Trajectory generation and control of a quadrotor with a cable-suspended load - A differentially-flat hybrid system. In *ICRA*, pages 4888–4895. IEEE, 2013.

[11] K. Sreenath, T. Lee, and V. Kumar. Geometric control and differential flatness of a quadrotor UAV with a cable-suspended load. In *52nd IEEE Conference on Decision and Control*, pages 2269–2274, Dec 2013.

[12] I. Palunko, R. Fierro, and P. Cruz. Trajectory generation for swing-free maneuvers of a quadrotor with suspended payload: A dynamic programming approach. In *IEEE ICRA*, pages 2691–2697, 2012.

[13] I. Palunko, P. Cruz, and R. Fierro. Agile load transportation. *IEEE Robotics Automation Magazine*, 19(3):69–79, 9 2012.

[14] S. Dai, T. Lee, and D. S. Bernstein. Adaptive control of a quadrotor UAV transporting a cable-suspended load with unknown mass. In *IEEE Conference on Decision and Control*, pages 6149–6154, 2014.

[15] P. Pereira, M. Herzog, and D. V. Dimarogonas. Slung load transportation with single aerial vehicle and disturbance removal. In *24th Mediterranean Conference on Control and Automation*, pages 671–676, 2016.

[16] M. Bisgaard, A. la Cour-Harbo, and J. D. Bendtsen. Adaptive control system for autonomous helicopter slung load operations. *Control Engineering Practice*, 18(7):800–811, 2010.

[17] N. Michael, J. Fink, and V. Kumar. Cooperative manipulation and transportation with aerial robots. *Autonomous Robots*, 30(1):73–86, 2011.

[18] G. Wu and K. Sreenath. Geometric control of multiple quadrotors transporting a rigid-body load. In *53rd IEEE Conference on Decision and Control*, pages 6141–6148, Dec 2014.

[19] T. Lee. Geometric control of multiple quadrotor UAVs transporting a cable-suspended rigid body. In *IEEE Conference on Decision and Control*, pages 6155–6160, 2014.

[20] I. Maza, K. Kondak, M. Bernard, and A. Ollero. Multi-UAV cooperation and control for load transportation and deployment. *Journal of Intelligent and Robotic Systems*, 57(1-4):417–449, 2010.

[21] P. E.I. Pounds, D.R. Bersak, and A.M. Dollar. Grasping from the air: Hovering capture and load stability. In *IEEE ICRA*, pages 2491–2498, May 2011.

[22] Pedro O. Pereira and Dimos V. Dimarogonas. Stability of load lifting by a quadrotor under attitude control delay. In *ICRA*, 2017 (to appear).